Biosensors and Bioelectronics 26 (2010) 815–821

Contents lists available at ScienceDirect

Biosensors and Bioelectronics

journal homepage: www.elsevier.com/locate/bios

Quartz crystal microbalance based nanosensor for lysozyme detection with lysozyme imprinted nanoparticles

Gulsu Sener[a,b], Erdogan Ozgur[a], Erkut Yılmaz[a], Lokman Uzun[a,*], Ridvan Say[c], Adil Denizli[a]

[a] Hacettepe University, Department of Chemistry, Ankara, Turkey
[b] Hacettepe University, Division of Nanotechnology and Nanomedicine, Ankara, Turkey
[c] Anadolu University, Department of Chemistry, Eskisehir, Turkey

ARTICLE INFO

Article history:
Received 17 February 2010
Received in revised form 1 June 2010
Accepted 4 June 2010
Available online 11 June 2010

Keywords:
QCM
Nanoparticles
Lysozyme
Molecular imprinting
Nanosensors

ABSTRACT

The aim of this study is to prepare quartz crystal microbalance (QCM) nanosensor for the real-time detection of lysozyme. In the first part, the lysozyme imprinted (MIP) nanoparticles were prepared by mini-emulsion polymerization. The MIP nanoparticles were characterized by TEM, zeta-sizer and FTIR–ATR measurements. Particle size was found around 50 nm. The MIP nanoparticles were attached by dropping of nanoparticle solution to gold surface and then, dried at 37 °C for 6 h. QCM nanosensor was characterized with AFM and ellipsometer. The observations indicated that the nanoparticle film was almost monolayer. The detection limit was found as 1.2 ng/mL. The specificity of the QCM nanosensor was shown by using albumin as a competitor molecule. The results show that the QCM nanosensor has high selectivity and sensitivity with a wide range of lysozyme concentrations in both aqueous solutions (0.2–1500 μg/mL) and natural sources (egg white) (460–1500 ng/mL).

1. Introduction

Lysozyme (EC 3.2.1.17), known as N-acetylmuramide glycanhydrolase, is a name of enzyme family which responds to catalyze a reaction as breaking the β1–4 bond found in peptidoglycan residues of bacterial cell walls between N-acetylmumaric acid and N-acetylglucosamine. Due to this property, lysozyme is called as body's own antibiotic. One of the main lysozyme sources is egg-white containing approximately 3.5% lysozyme. Lysozyme is a relatively small protein (MW: 14.3 kDa) consists of only 129 amino acid residues and has an isoelectric point of 11.0. Due to its small size and simple molecular structure, lysozyme has been chosen as a unique model protein in developing of new detection methods. There are several benchmark lysozyme detection methods in order to detect lysozyme molecules. Determination of lytic activity by *Micrococcus lysodeikticus* cells and enzyme linked immunosorbent assays (ELISA) are mostly applied methods (Liao et al., 2001). These methods have some drawbacks such as low detection limit, impossibility of routine analysis inaccurate quantification due to interfering substances. Although ELISA is promising method because of low detection limit, high specificity and sensitivity, unexpected cross-reactivity high cast and low shelf-life of the assay are still waiting for the solution (Vidal et al., 2005; Van Hengel, 2007). Change in lysozyme amount can be a former marker of some health problems. Porstmann et al. (1989) reported that lysozyme concentration in cerebrospinal fluid increased in meningitis patients (Porstmann et al., 1989). In addition, it was reported that lysozyme concentration in serum and urine increased in case of leukemia (Pascual et al., 1973) and several kidney problems (Horpacsy et al., 1978). According to Serra et al. (2002) lysozyme may be a new prognostic factor in patients with breast cancer (Serra et al., 2002). Recently, antibodies against to citrullinated variants of lysozyme were found in rheumatoid arthritis patients (Ireland et al., 2006). Therefore, detection of lysozyme has been getting importance and developing new, rapid, cheap and effective biosensors have been under investigation.

Quartz crystal microbalance (QCM) biosensors, member of mass-sensitive chemical sensors, have been getting researchers' attention because of their properties such as high selectivity, low cost, portability, stability and simplicity (Wu and Syu, 2006). The QCM allows dynamic monitoring of biochemical interactions, using an oscillating crystal with the biomolecules immobilized on its surface. The increased mass, associated with the binding reaction, results in a decrease of the oscillating frequency (Diltemiz et al., 2009). Recently, QCM-based biosensors have been used in the detection of several analytes such as clinical targets (Chou et al., 2002), environmental contaminants (Fung and Wong, 2001), marker of genetic diseases (Feng et al., 2007), determination of oxidative stress (Ersöz et al., 2009; Say et al., 2009), quantification of protein (Lin et al., 2004), detection of genetically modified organ-

* Corresponding author at: Hacettepe University, Department of Chemistry, Biochemistry Division Beytepe, 06532 Ankara, Turkey. Tel.: +90 312 2977963; fax: +90 312 2992163.
E-mail address: lokman@hacettepe.edu.tr (L. Uzun).

0956-5663/$ – see front matter © 2010 Elsevier B.V. All rights reserved.
doi:10.1016/j.bios.2010.06.003

isms (GMOs) (Mannelli et al., 2003) and bimolecular interactions (Svedhem et al., 2003).

In order to create sensitive QCM sensor surface, although several methods can be applied, the most promising approach is molecular imprinting technique. The methodology, mainly depends on the molecular recognition, is a type of polymerization which occurs around the interested molecules called as template and creates specific cavities in the highly cross-linked polymeric matrices (Ozcan et al., 2006). Molecular imprinted polymers (MIPs) have been used in several applications such as artificial enzymes (Toorisaka et al., 1999), advanced materials for solid-phase extraction (Esen et al., 2009), protein purification (Bereli et al., 2008; Uzun et al., 2009a), affinity detoxification (Andaç et al., 2004; Asir et al., 2005), and sensing materials for sensor devices (Diltemiz et al., 2009; Say et al., 2009; Uzun et al., 2009b).

Conventional imprinting process has some drawbacks. First of all, imprinted polymers are generally prepared via bulk polymerization; then, crashed into small particles. Therefore, the imprinted cavities in the polymeric structure may be formed heterogeneously (Tan et al., 2008). Secondly, formed cavities can be obtained deep inside of the structure. So, the template molecules cannot be completely removed from there and irregular adsorption rate can be occurred (Turner et al., 2006; Bossi et al., 2007). In order to solve these problems, nanotechnology serves a novel approach which is imprinting into nanoparticles. When imprinting of the template molecules into nanoparticles, more homogeneously distributed imprinted cavities can be obtained surface or near inside of the nanoparticles (Hayden et al., 2006; Bonini et al., 2007). Hereby, the template molecules can be removed easily and higher adsorption rate can be obtained. In addition, because of almost complete removal of the template molecule, the amounts of specific cavities are getting more (Li et al., 2006). Hence, higher adsorption capacities and rates can be achieved.

In this study, we aimed to prepare QCM nanosensor using lysozyme imprinted nanoparticles. For this purpose, firstly, we prepared N-methacryloyl-L-histidine methylester (MAH) as a functional monomer. Then, the lysozyme imprinted poly(ethylene glycol dimethacrylate-N-methacryloyl-L-histidine methylester) (PEDMAH) nanoparticles were synthesized via mini-emulsion polymerization. The nanoparticles were attached on the QCM sensor surface. Lysozyme detection studies were carried out using aqueous lysozyme solutions and natural lysozyme source, chicken egg white, in different concentrations. Kinetic and isotherm parameters were calculated by applying association kinetics analysis, Scatchard, Langmuir, Freundlich and Langmuir–Freundlich isotherms.

2. Materials and methods

2.1. Materials

Lysozyme (EC 3.2.1.17), albumin (bovine serum), L-histidine methyl ester, poly(vinyl alcohol) (PVA), sodium dodecyl sulfate (SDS), ammonium persulfate, sodium bicarbonate, sodium bisulfite and potassium bromide (FTIR grade) were obtained from Sigma Chemical Co. (St. Louis, USA). Ethylene glycol dimethacrylate and absolute methanol were purchased from Fluka A.G. (Buchs, Switzerland). All other chemicals were of reagent grade and purchased from Merck A.G. (Darmstadt, Germany).

2.2. Synthesis of N-methacryloyl-L-histidine methyl ester (MAH) monomer

The following experimental procedure was applied for the synthesis of N-methacryloyl-L-histidine methyl ester (MAH) (Garipcan and Denizli, 2002). L-Histidine methyl ester (5.0 g) and hydroquinone (0.2 g) were dissolved in 100 mL of dichloromethane solution. This solution was cooled down to 0 °C. Triethylamine (12.7 g) was added to the solution. Methacryloyl chloride (5.0 mL) was poured slowly into this solution and then it was stirred magnetically at room temperature for 2 h. At the end of the chemical reaction period, hydroquinone and unreacted methacryloyl chloride were extracted with 10% NaOH solution. Aqueous phase was evaporated in a rotary evaporator. The residue (i.e., MAH) was crystallized in NaOH solution (10%, w/w).

MAH was characterized by ^{1}H NMR. The obtained peaks in the spectrum are listed as ^{1}H NMR (400 MHz, DMSO-d_6, δ): 1.85 (t; 3H, CH_3), 1.4 (m; 2H, CH_2), 3.42 (s; 3H, $-OCH_3$), 5.28 (s; 1H, vinyl H), 5.6 (s; 1H, vinyl H), 6.6–6.9 (m; 5H, aromatic); 7.42 (1H, NH); δ 7.47 (1H, NH).

2.3. Preparation of lysozyme imprinted PEDMAH nanoparticles

Lysozyme imprinted poly(ethylene glycol dimethacrylate-N-methacryloyl-L-histidine methyl ester) (PEDMAH) nanoparticles were prepared by two phase mini-emulsion polymerization method. Before polymerization two different aqueous phases were prepared. The first aqueous phase was prepared by dissolving of PVA (200 mg), SDS (30 mg) and sodium bicarbonate (25 mg) in 10 mL deionized water. The second phase was prepared by dissolving of PVA (100 mg) and SDS (100 mg) in 200 mL of deionized water. MAH (5 mg) was dissolved in ethylene glycol dimethacrylate (2.1 mL) to form organic phase. The organic phase was slowly added to the first aqueous phase. In order to obtain mini-emulsion, the mixture was homogenized at 25,000 rpm by a homogenizer (T10, Ika Labortechnik, Germany). After homogenization, the template molecule (lysozyme, 100 mmol) was added to mini-emulsion and the mixture was stirred to obtain effectively interacted monomer-template pre-polymerization complex for 2 h. Then, the mixture was slowly added to the second aqueous phase while the phase has been stirring in a sealed-cylindrical polymerization reactor (250 mL). The reactor was magnetically stirred at 300 rpm (Radleys Carousel 6, UK). The polymerization mixture was slowly heated to 40 °C, polymerization temperature. After that, nitrogen gas was bubbled through the solution for removing of dissolved oxygen for 5 min. Then, initiators, sodium bisulfite (125 mg) and ammonium persulfate (125 mg), were added into the solution. Polymerization was continued at 40 °C for 24 h. The lysozyme imprinted nanoparticles were washed with water and water/ethyl alcohol mixtures, in order to remove unreacted monomers, surfactant and initiator. For each washing step, the solution was centrifuged at 30,000 rpm for 30 min (Allegra-64R Beckman Coulter, USA); then, the nanoparticles were dispersed in fresh washing solution. After last washing step, the lysozyme imprinted nanoparticles were dispersed in deionized water containing 0.3% sodium azide and stored at 4 °C.

2.4. Characterization of lysozyme imprinted PEDMAH nanoparticles

Characterization of the nanoparticles was done by zeta-sizer, TEM and FTIR–ATR measurements. The experimental procedure for zeta-sizer as follows briefly: nanoparticles sample (dispersion in 3 mL deionized water) was immersed into sample holder of the zeta-sizer (NanoS, Malvern Instruments, London, UK). Light scattering was done at incidence angle 90° and 25 °. For data analysis, density and refraction index of deionized water were used as 0.88 mPa s and 1.33, respectively. Light scattering signal was calculated as nanoparticle number per second. Here, we have to say that nanoparticle concentration in the sample was enough for measurement. For TEM analysis, the imprinted nanoparticle sample was dropped onto carbon coated copper grid and then dried

at room temperature. TEM micrographs were taken at 200 kV by TEM microscope (FEI, Tecnai G2 F30, Oregon, USA). For FTIR–ATR measurement, the lysozyme imprinted nanoparticles (2 mg) were mixed with potassium bromide (98 mg); then, mixture was crushed until obtaining fine powder. The powder was pressed into a pellet form and, then, the FTIR spectrum was recorded. The pellet was put into sample holder of FTIR–ATR spectrophotometer (Thermo Fisher Scientific, Nicolet iS10, Waltham, MA, USA) and total light reflection from surface was measured in the wavenumber range of 650–4000 cm^{-1} at 2 cm^{-1} resolution. Eighteen replicate FTIR–ATR spectra were obtained and baseline correction was done due to Ge window.

2.5. Preparation of lysozyme imprinted QCM nanosensor

Before attachment of the lysozyme imprinted nanoparticles onto the QCM sensor surface, gold surface of the sensor was cleaned with acidic piranha solution (3:1 H_2SO_4:H_2O_2, v/v). The sensor was immersed in 20 mL of acidic piranha solution for 30 s. Then, it was washed with pure ethyl alcohol and dried in vacuum oven (200 mmHg, 40 °C) for 3 h. In order to attach the lysozyme imprinted nanoparticles onto the QCM sensor, an aliquot (5 μl) of nanoparticles dispersion (4.2%, v/v) was dropped on the gold surface of the QCM sensor. Then, the sensor was dried in oven (37 °C, 6 h). Finally, the lysozyme imprinted QCM nanosensor was washed three times with both water and ethyl alcohol and dried with nitrogen gas under vacuum (200 mmHg, 40 °C).

2.6. Template removal from nanosensor

There are cooperative interactions originated from secondary forces between MAH and lysozyme molecules. But, more dominated electrostatic interactions and hydrogen bonding occurred between imidazole group of MAH monomer and polar groups of side chain of lysozyme molecules. In order to remove template molecule lysozyme, these interactions should be broken. For this purpose, we used 1 M NaCl solution (pH 8.0, phosphate buffer) as a desorption agent. The first template removal study was carried out via batch system. Lysozyme imprinted QCM nanosensor was immersed into desorption solution (20 mL). The nanosensor was shaked in bath (200 rpm) at room temperature. After lysozyme removal, the nanosensor was washed with deionized water and dried with nitrogen gas under vacuum (200 mmHg, 25 °C).

2.7. Characterization of lysozyme imprinted QCM nanosensor

Characterization studies of lysozyme imprinted QCM nanosensor were done by using AFM and ellipsometer. AFM observations were carried out by using AFM (Nanomagnetics Instruments, Oxford, UK) in tapping mode. AFM system makes measurement in high resolution (i.e., 4096 × 4096 pixels) because of free cantilever interferometer. Lysozyme imprinted QCM nanosensor was attached on a sample holder by using double-side carbon strip. Observation study was carried out via tapping mode in air atmosphere. Applied experimental parameters were oscillation frequency (341.30 Hz), vibration amplitude (1 V_{RMS}) and free vibration amplitude (2 V_{RMS}). Samples were scanned with 2 μm/s scanning rate and 256 × 256 pixels resolution to obtain view of 2 μm × 2 μm area.

Ellipsometer measurements were carried out by using an auto-nulling imaging ellipsometer (Nanofilm EP3, Germany). All thickness measurements have been performed at a wavelength of 532 nm with an angle of incidence of 72°. In the layer thickness analysis, a four-zone auto-nulling procedure integrating over a sample area of approximately 50 μm × 50 μm followed by a fitting algorithm has been performed. In order to analysis of size of lysozyme imprinted nanoparticles, a four-phase model, air/nanoparticle/gold/quartz crystal, was assumed. Measurement was carried out as triplicate 6 different points of nanosensor surface and the results were reported as mean value of the measurements with standard deviations.

2.8. Monitoring of lysozyme imprinted QCM nanosensor response

The lysozyme imprinted QCM nanosensor, was used for real-time detection of lysozyme from aqueous solution. For this purpose, a QCM system (RQCM, INFICON Acquires Maxtek Inc., New York, USA) was used. The applied experimental procedure can be briefly summarized as: the lysozyme imprinted QCM nanosensor was sequentially washed with sodium hydroxide (50 mL, 2.0 mL/min flow-rate), deionized water (50 mL, 2.0 mL/min flow-rate), and equilibration buffer (pH:7.4 phosphate buffer, 50 mL, 2.0 mL/min flow-rate). Then, the lysozyme imprinted QCM nanosensor response was monitored until it reached stable frequency. After that, aqueous lysozyme solutions (pH: 7.4 phosphate buffer; 25 mL; 2.0 mL/min flow-rate) in different concentrations in the range of 0.2 μg/mL–1500 μg/mL were applied to the lysozyme imprinted QCM nanosensor and frequency shifts were monitored and evaluations were repeated as triplicate. Then, desorption was done by applying 10 mL of 1 M NaCl solution (in pH 8.0 phosphate buffer, 20 mM) with 1.0 mL/min flow-rate. After desorption step, the lysozyme imprinted QCM nanosensor was washed with deionized water and equilibration buffer. For each lysozyme sample application, adsorption–desorption-cleaning steps were repeated.

Lysozyme detection from natural source was also carried out by using freshly prepared chicken egg white. For this purpose, chicken egg white was separated from fresh eggs and diluted to 50% (v/v) with phosphate buffer (100 mM, pH 7.4). The diluted egg-white was homogenized in an ice bath and centrifuged at 4 °C, at 10,000 rpm for 30 min. Freshly prepared chicken egg white samples were diluted in different ratios between 1/3333 and 1/10000. QCM nanosensor responses were determined as given above. In order to show specificity and selectivity of lysozyme imprinted QCM nanosensor, the response of the nanosensor was monitored while applying albumin and albumin/lysozyme solutions.

3. Results and discussion

3.1. Preparation and characterization of lysozyme imprinted QCM nanosensor

The lysozyme imprinted nanoparticles were prepared by mini-emulsion polymerization. In order to determine particle size and size distribution of the nanoparticles, zeta-sizer and transmission electron microscopy (TEM) were used. The results obtained from zeta-sizer show that the lysozyme imprinted nanoparticles have average particle size as 51.2 nm with a polydispersity around 0.17 (Fig. SI1a). TEM photo of the nanoparticles also confirms the result. The TEM observation showed that the nanoparticles have spherical shape and monosize around 50 nm (Fig. SI1b). Therefore, we can conclude that applied polymerization recipe was suitable for synthesizing of the monosize nanoparticles. Preparation of the monosize nanoparticles is an important step which determines adsorption behavior and controls homogeneity of the imprinted cavities.

The imprinted nanoparticles were also characterized by FTIR–ATR (Fig. SI1c). In the spectrum, aliphatic –CH band at 2940 cm^{-1} and carbonyl band at 1730 cm^{-1} were determined. Also, amide bands originated from functional monomer, MAH, were determined at 1458 cm^{-1} and 1370 cm^{-1}, respectively. Amine stretching bands were determined at 3671 cm^{-1} and 3736 cm^{-1},

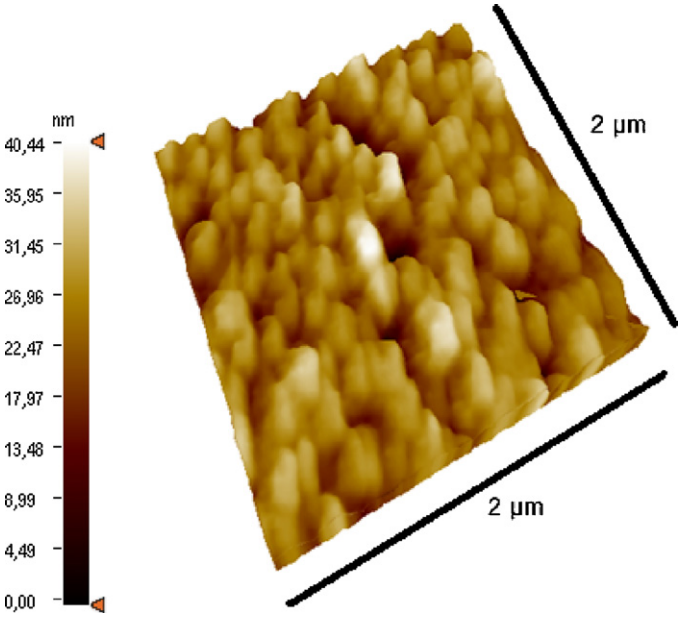

Fig. 1. Atomic force microscopy picture of lysozyme imprinted QCM sensor.

respectively. The most interesting band determined in the spectrum is the band at 1145 cm^{-1} which was stemmed from imidazole ring of the MAH. The high intensity of the band approximately, half of the carbonyl band, shows that the functional monomer, in other word imprinted cavities, is oriented toward to the surface. Therefore, we can say that the imprinted cavities of the nanoparticles are on the surface which is one of the important parameters for achieving rapid and efficient lysozyme detection.

After attachment of the nanoparticles onto the sensor surface, QCM nanosensor was characterized by atomic force microscopy (AFM) and ellipsometry. The lysozyme imprinted QCM nanosensor was characterized by AFM (Fig. 1). Surface deepness determined by AFM measurements of the lysozyme imprinted QCM nanosensor is 40.4 nm. The results are well fitted to the data of zeta-sizer measurement and TEM analysis. AFM image also shows that the nanoparticles were almost homogeneously attached on the surface of QCM sensor. In order to prove this situation, ellipsometry analysis was also carried out and coherency is seen between AFM and ellipsometer measurements. Surface deepness obtained from ellipsometer of the lysozyme imprinted QCM nanosensor is 44.04 ± 2.75 nm, respectively. As a conclusion, we can say that homogeneous and monolayer attachment of the nanoparticles has been accomplished.

3.2. *Real-time monitoring of lysozyme imprinted QCM nanosensor response*

QCM biosensor has attracted great interests for producing novel detection platforms (Diltemiz et al., 2009). Molecular imprinting approach is one of the applied popular methodologies for this purpose. Conventional imprinting method has some limiting problems mentioned before. Therefore, recent attempts depended on imprinting into/onto nanoparticles have been investigated. This approach serves a unique solution for obtaining homogeneous distribution of imprinted nanocavities, rapid and more selective detection, high specificity and reproducibility etc. In addition, imprinting into nanoparticles increases imprinted surface area and amount of nanocavities (Fig. SI2). When imprinted nanoparticles attached onto sensor surface in proper orientation, homogeneously distributed specific interaction sites and higher amount of

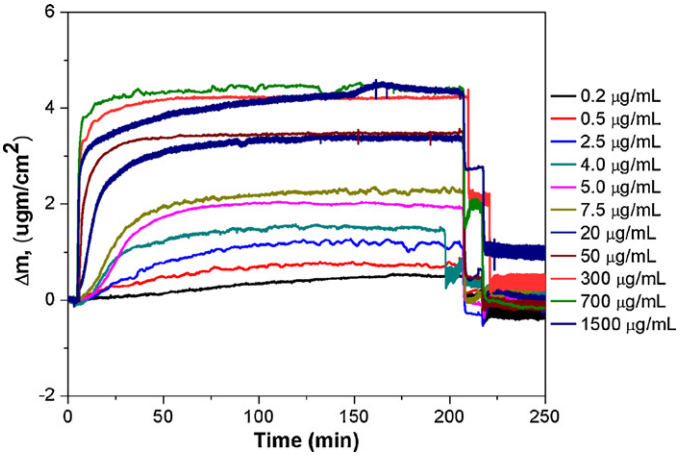

Fig. 2. Real-time lysozyme detection with lysozyme imprinted QCM nanosensor.

imprinted nanocavities per unit sensor area can be obtained. Rapid and selective interactions between analyte, imprinted molecule, and sensor surface can be achieved (Reimhult et al., 2008).

In this study, the lysozyme imprinted nanoparticles were used to produce QCM nanosensor for real-time lysozyme detection from both aqueous solutions and natural lysozyme source, chicken egg-white. For this purpose, the sensor was firstly interacted with aqueous lysozyme solutions in different concentrations in the range of 0.2–1500 µg/mL. Fig. 2 shows real-time change in lysozyme detection response of QCM nanosensor with respect to time. As seen in the figure, QCM nanosensor shows a quick response to lysozyme molecules. QCM nanosensor response was started as soon as lysozyme solution reached to the sensor surface. The increase in concentration caused also increase in QCM nanosensor response. The results depend on concentration gradient between aqueous phase, lysozyme solution, and solid-phase, lysozyme imprinted QCM nanosensor surface. Nanosensor response firstly increased linearly; then, reached platue value around relatively high lysozyme concentration (300 µg/mL) because of saturation of accessible imprinted nanocavities.

Fig. 3 shows the relationship between mass shift and lysozyme concentration (Fig. SI3). As seen in the figure, lysozyme imprinted QCM nanosensor shows a linearity in a wide concentration range of 0.2 µg/mL–100 µg/mL. Then, slope of the curve declined because of saturation of lysozyme imprinted nanocavities. After

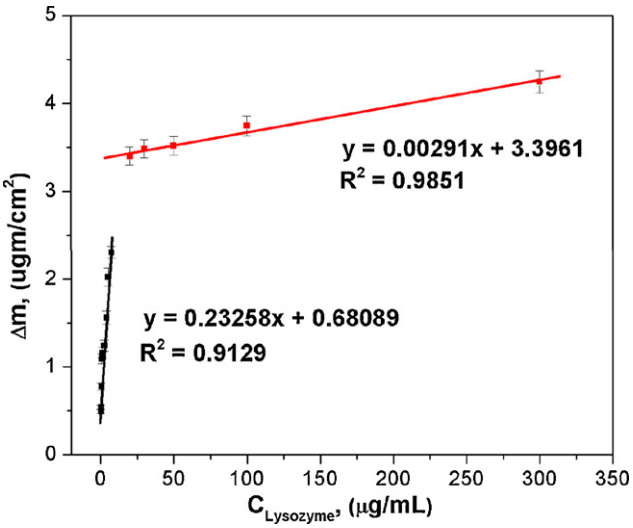

Fig. 3. Concentration dependency of lysozyme imprinted QCM nanosensor.

Table 1
Kinetic and isotherm parameters.

Association kinetics analysis		Equilibrium analysis (Scatchard)		Langmuir		Freundlich		Langmuir–Freundlich	
k_a(μg/mLs)	1.013×10^{-4}	Δm_{max}(μg/cm^2)	4.327	Δm_{max} μg/cm^2	4.259	Δm_{max} μg/cm^2	1.474	Δm_{max} μg/cm^2	24.43
k_d(1/s)	0.0049	K_A(μg/mL)	0.1539	K_A μg/mL	6.208	1/n	0.184	1/n	0.184
K_A(μg/mL)	0.0206	K_D(mL/μg)	6.498	K_D mL/μg	0.161	R^2	0.8028	K_A μg/mL	32.95
K_D(mL/μg)	48.38	R^2	0.9616	R^2	0.9884			K_D mL/μg	0.0303
R^2	0.9403							R^2	0.7905

lysozyme concentration of 750 μg/mL, the lysozyme imprinted QCM nanosensor response goes almost constantly. As seen in figures, the lysozyme imprinted QCM nanosensor has two different linear regions for aqueous lysozyme solutions. The result shows that lysozyme molecules bound to the lysozyme imprinted QCM nanosensor through two different orientations with high affinity. The results mainly depend on the spherical structure of imprinted nanoparticles. When the imprinted nanoparticles were attached on the sensor surface, some of the imprinted nanocavities were sterically closed. Therefore, lysozyme molecules cannot reach these nanocavities as easily as upper nanocavities; but still have high affinity to them (Fig. SI2).

3.3. Mathematical analysis of lysozyme imprinted QCM nanosensor data

QCM nanosensor data were analyzed for the determination of kinetic and equilibrium isotherm parameters such as forward and reverse binding constants, k_a (μg/mL s) and k_d (1/s), forward and reverse equilibrium constants, K_A (μg/mL) and K_D (mL/μg). For this purpose, pseudo- first- order kinetic analysis and four different equilibrium isotherm models, Scatchard, Langmuir, Freundlich, and Langmuir–Freundlich, were applied to the lysozyme imprinted QCM nanosensor data (Lin et al., 2005; Uzun et al., 2009b). Linear form of applied model can be given as:

$$\text{Equilibrium Kinetic Analysis}: \quad \frac{d\Delta m}{dt} = k_a C \Delta m_{max} - (k_a C + k_d)\Delta m \tag{1}$$

$$\text{Scatchard}: \quad \frac{\Delta m_{ex}}{C} = K_A(\Delta m_{max} - \Delta m_{eq}) \tag{2}$$

$$\text{Langmuir}: \quad \Delta m = \left\{ \frac{\Delta m_{max} C}{K_D + C} \right\} \tag{3}$$

$$\text{Freundlich}: \quad \Delta m = \Delta m_{max} C^{1/n} \tag{4}$$

$$\text{Langmuir–Freundlich}: \quad \Delta m = \left\{ \frac{\Delta m_{max} C^{1/n}}{K_D + C^{1/n}} \right\} \tag{5}$$

where Δm is amount of increased mass on unit area of QCM nanosensor (μg/cm^2); C is concentration of lysozyme solution (μg/mL); 1/n is Freundlich exponent; k_a (μg/mL) and k_d (1/s) are forward and reverse kinetic rate constants; K_A (μg/mL) and K_D (mL/μg) are forward and reverse equilibrium constants; subscripts ex, max and eq indicate experimental, maximum and equilibrium, respectively. Here, we have to note that some transformations from capacity (Q) to Δm have been done to avoid conversion of unit improperly. In addition; when applying equilibrium kinetic analysis, we have calculated slopes of curves and plotted to concentration vs. slope curve to determination of k_a and k_d values, respectively (Uzun et al., 2009b).

In order to determine the homogeneity of imprinted materials, the adsorption models can be applied to adsorption data. Langmuir model depends on the acceptation of homogeneous distribution of interaction points with similar energy and no lateral interactions. Freundlich model is well fitted to heterogeneous surfaces. Mixed model, Langmuir–Freundlich can be applied to a system that is not full fitted to both systems, provides heterogeneity information adsorption behavior over wide concentration regions (Fig. SI4).

Both models, Scathard (R^2: 0.962) and Langmuir models (R^2: 0.988), have high correlation coefficients. The linearity of the Langmuir equation was better than that of Scatchard equation, which means that the binding of lysozyme molecules onto lysozyme imprinted QCM nanosensor is monolayer (Wei et al., 2005; Li and Husson, 2006; Uzun et al., 2009b). Freundlich model is used to show multilayer binding of analyte molecules. Linear regression coefficients of Freundlich and Langmuir–Freundlich isotherms were 0.8028 and 0.7905, respectively. The results indicate the poor agreement with these isotherm equations and consolidate monolayer adsorption of lysozyme molecules onto QCM nanosensor surface. The calculated parameters for all models were given in Table 1.

The best fitted model to explain the interaction between the lysozyme imprinted QCM nanosensor and lysozyme molecules is Langmuir isotherm. The Δm_{max} value calculated by using Langmuir model was very close to the experimental one (4.58). Due to the result, K_A and K_D values were determined as 0.161 μg/mL and 6.208 mL/μg, respectively. Detection limit, defined as the concentration of analyte giving frequency shift equivalent to three standard deviation of the blank, was determined as 1.2 ng/mL.

3.4. Specificity and selectivity of lysozyme imprinted QCM nanosensor

The lysozyme imprinted QCM nanosensor was also used to detect lysozyme molecules in natural lysozyme source, chicken egg white. Chicken egg white, contains approximately 3.5% lysozyme, samples were interacted with lysozyme imprinted QCM nanosensor. For this purpose, freshly prepared chicken egg white samples were diluted in different ratios in the range of 1/3333–1/10000. Mass shift obtained from chicken egg white samples were given in Fig. 4a. As seen from the figure, decrease in dilution ratio, increase in concentration, caused increase in nanosensor response as expected. The lysozyme imprinted QCM nanosensor showed a response when egg white samples were diluted in high ratio as 10,000 times, lysozyme concentration was approximately 460 ng/mL. As a conclusion, lysozyme imprinted QCM nanosensor has an ability to detect lysozyme in a natural complex mixture such as, chicken egg white.

In order to show selectivity of lysozyme imprinted QCM nanosensor, real-time albumin detection was also carried out (Fig. 4b). For this purpose albumin solution (1.0 μg/mL, pH:7.4, phosphate buffer) was applied to QCM nanosensor. As seen from the figure, QCM nanosensor did not give any response to albumin solution. As a second confirmation of selectivity of QCM nanosensor, we have applied the solution containing albumin (1.0 μg/mL) and lysozyme (1.0 μg/mL) to QCM nanosensor (Fig. 4c). As seen from the figure lysozyme imprinted QCM nanosensor has a response as the solution containing just lysozyme. It also shows that lysozyme imprinted QCM nanosensor specifically detects lysozyme molecule in not only single component solution but also competitive manner.

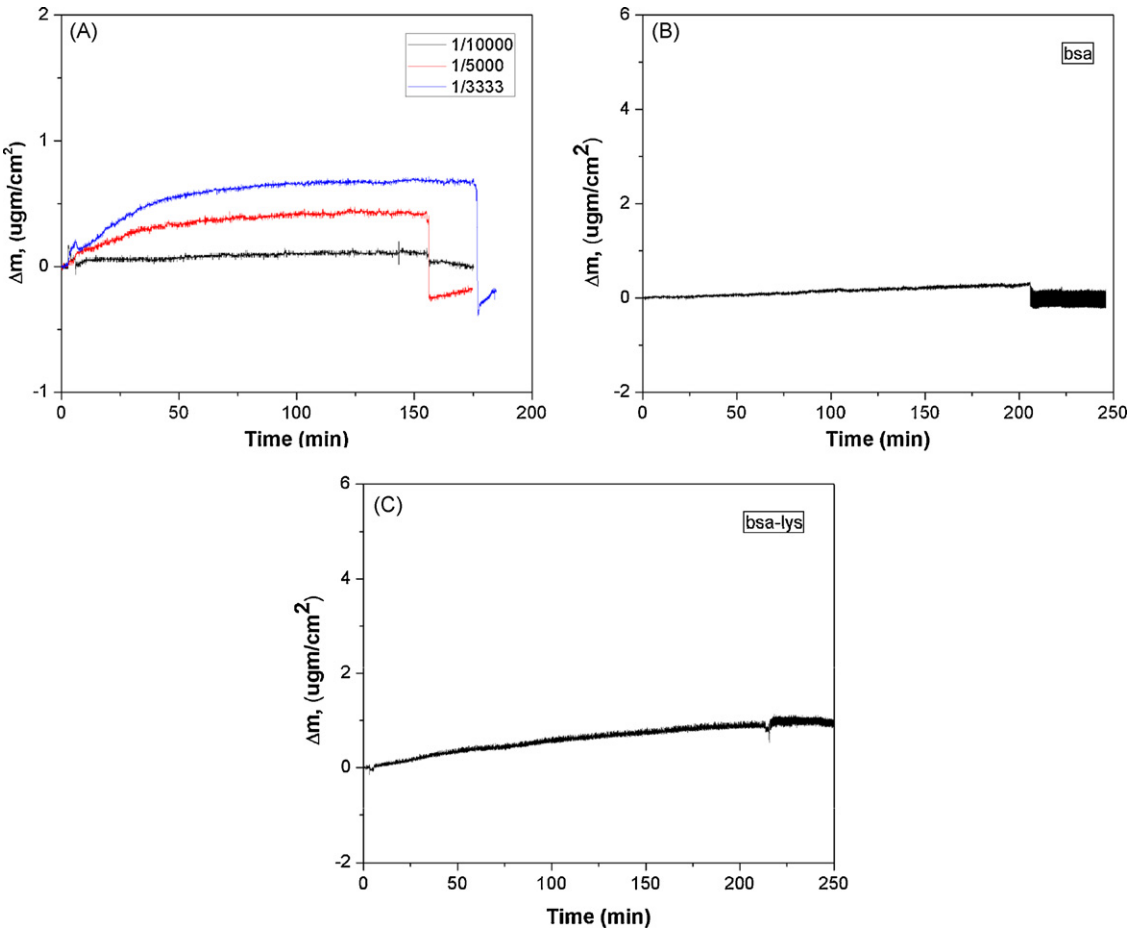

Fig. 4. Specificity of lysozyme imprinted QCM nanosensor. (A) real-time lysozyme detection from natural source in different dilutions; (B) real-time albumin response from single component aqueous solution; (C) real-time QCM response from aqueous solution containing albumin/lysozyme mixture.

3.5. Reproducibility

In order to show the reproducibility of lysozyme imprinted QCM nanosensor response, four equilibration-adsorption-regeneration cycles were repeated by aqueous lysozyme solution, 0.5 μg/mL (Fig. 5). As seen in the figure, lysozyme imprinted QCM nanosensor has shown reproducible mass shift during the cycles.

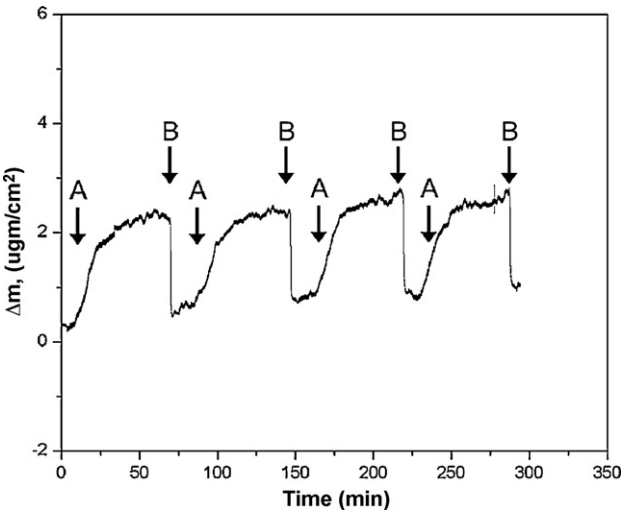

Fig. 5. Reproducibility of lysozyme imprinted QCM nanosensor response. (A) Adsorption; (B) Desorption.

4. Conclusion

In the present study, we prepared quartz crystal microbalance (QCM) nanosensor for real time lysozyme detection. QCM nanosensor was prepared by modification of the gold surface of QCM sensor with the lysozyme imprinted PEDMAH nanoparticles. The lysozyme imprinted (MIP) nanoparticles were prepared by mini-emulsion polymerization reaction of MAH and EGDMA in the presence of lysozyme. The MIP nanoparticles were characterized by TEM, zeta-sizer and FTIR–ATR measurements. Particle size was found around 50 nm. The MIP nanoparticles were attached by dropping of nanoparticle solution to gold surface and then, dried at 37 °C for 6 h. QCM nanosensor was characterized with AFM and ellipsometer. The observations indicated that the nanoparticle film was almost monolayer. The detection limit was found as 1.2 ng/mL. The results show that the MIP nanosensor has high selectivity and sensitivity towards both aqueous solutions and natural sources (chicken egg white) at a wide range of concentrations (0.2–1500 μg/mL).

Appendix A. Supplementary data

Supplementary data associated with this article can be found, in the online version, at doi:10.1016/j.bios.2010.06.003.

References

Andaç, M., Say, R., Denizli, A., 2004. J. Chromatogr. B 811 (2), 119–126.
Asir, S., Uzun, L., Turkmen, D., Say, R., Denizli, A., 2005. Sci. Technol. 40 (September), 3167–3185.

Bereli, N., Andaç, M., Baydemir, G., Say, R., Galaev, I.Y., Denizli, A., 2008. J. Chromatogr. A 1190 (1–2), 18–26.
Bonini, F., Piletsky, S., Turner, A.P.F., Speghini, A., Bossi, A., 2007. Biosens. Bioelectron. 22, 2322–2328.
Bossi, A., Bonini, F., Turner, A.P.F., Piletsky, S.A., 2007. Biosens. Bioelectron. 22, 1131–1137.
Chou, S., Hsu, W., Hwang, J., Chen, C., 2002. Anal. Chim. Acta 453 (2), 181–189.
Diltemiz, S.E., Hür, D., Ersöz, A., Denizli, A., Say, R., 2009. Biosens. Bielectron. 25 (3), 599–603.
Ersöz, A., Diltemiz, S.E., Özcan, A.A., Denizli, A., Say, R., 2009. Sens. Actuators B 137, 7–11.
Esen, C., Andac, M., Bereli, N., Say, R., Henden, E., Denizli, A., 2009. Mater. Sci. Eng. C 29 (8), 2464–2470.
Feng, K., Li, J., Jiang, J., Shen, G., Yu, R., 2007. Biosens. Bioelectron. 22 (8), 1651–1657.
Fung, Y.S., Wong, Y.Y., 2001. Anal. Chem. 73, 5302–5309.
Garipcan, B., Denizli, A., 2002. Macromol. Biosci. 2 (3), 135–144.
Hayden, O., Haderspöck, C., Krassnig, S., Chen, X., Dickert, F.L., 2006. Analyst 131, 1044–1050.
Horpacsy, G., Zinsmeyer, J., Schroder, K., Mebel, M., 1978. Clin. Chem. 24, 74–79.
Ireland, J., Herzog, J., Unanue, E.R., 2006. J. Immunol. 177, 1421–1425.
Li, X., Husson, S.M., 2006. Biosens. Bioelectron. 22, 336–348.
Li, Z., Ding, J., Day, M., Tao, Y., 2006. Macromolecules 39, 2629–2636.
Liao, Y.H., Brown M.B., Martin G.P., 2001. J. Pharm. Pharmacol. 53, 549–554.
Lin, L.P., Huang, L.S., Lin, C.W., Lee, C.K., Chen, J.L., Hsu, S.M., Lin, S., 2005. Cur. Drug Target 5, 61–72.
Lin, T.Y., Hu, C.H., Chou, T.C., 2004. Biosens. Bioelectron. 20, 75–81.
Mannelli, I., Minunni, M., Tombelli, S., Mascini, M., 2003. Biosens. Bioelectron. 18, 129–140.
Ozcan, A.A., Say, R., Denizli, A., Ersoz, A., 2006. Anal. Chem. 78, 7253–7258.
Pascual, R., Gee, J., Finch, S., 1973. N. Eng. J. Med. 289, 1074–11074.
Porstmann, B., Jung, K., Schmechta, H., Evers, U., 1989. Clin. Biochem. 22, 349–355.
Reimhult, K., Yoshimatsu, K., Risveden, K., Chen, S., Ye, L., Krozer, A., 2008. Biosens. Bioelctron. 23, 1908–1914.
Say, R., Gultekin, A., Özcan, A.A., Denizli, A., Ersöz, A., 2009. Anal. Chim. Acta 640, 82–86.
Serra, C., Vizoso, F., Alonso, L., Rodríguez, J.C., González, L.O., Fernández, M., Lamelas, M.L., Sánchez, L.M., García-Muñiz, J.L., Baltasar, A., Medrano, J., 2002. Breast Cancer Res. 4, R16.
Svedhem, S., Dahlborg, D., Ekeroth, J., Kelly, J., Höök, F., Gold, J., 2003. Langmuir 19, 6730–6736.
Tan, C.J., Wangrangsimakul, S., Bai, R., Tong, Y.W., 2008. Chem. Mater. 20 (1), 118–127.
Toorisaka, E., Yoshida, M., Uezu, K., Goto, M., Furusaki, S., 1999. Chem. Lett. 5, 387–388.
Turner, N.W., Jeans, C.W., Brain, K.R., Allender, C.J., Hlady, V., Britt, D.W., 2006. Biotechnol. Prog. 22, 1474–1489.
Uzun, L., Say, R., Ünal, S., Denizli, A., 2009a. J. Chromatogr. B 877, 181–188.
Uzun, L., Say, R., Ünal, S., Denizli, A., 2009b. Biosens. Bioelectron. 24, 2878–2884.
Vidal, M.L., Gautron, J., Nys, Y., 2005. J. Agric. Food. Chem. 53, 2379–2385.
Van Hengel, A.J., 2007. Anal. Bioanal. Chem. 389, 111–118.
Wei, X., Samadi, A., Husson, S.M., 2005. Sci. Technol. 40 (Sep), 109–129.
Wu, A.H., Syu, M.J., 2006. Biosens. Bielectron. 21, 2345–2353.